JOURNAL OF GEOPHYSICAL RESEARCH, VOL. 92, NO. A8, PAGES 8595-8602, AUGUST 1, 1987

Interpretation of Electrostatic Noise Observed by Voyager 1 in Titan's Wake

T. Z. MA, D. A. GURNETT, AND C. K. GOERTZ

Department of Physics and Astronomy, The University of Iowa, Iowa City

During the Voyager 1 spacecraft flyby of Titan on November 12, 1980, an intense band of low-frequency electric field noise was observed during the inbound wake crossing. This analysis shows that the noise is generated by a beam-plasma interaction between the corotating magnetosphere of Saturn and newly created ions from the atmosphere of Titan. The analysis is based on plasma and wave measurements from Voyager 1 and reasonable assumptions. The results agree quite well with the observation. The analysis shows that the instability only occurs where the density of the corotational ions is comparable to the density of ions originating from Titan's atmosphere. The growth rate is high enough to generate the observed noise, and the calculated and observed frequency ranges are in good agreement. The asymmetry between the intensities in the inbound and outbound wake are explained by a simple model for the trajectories of ions from Titan's atmosphere.

1. INTRODUCTION

During the Voyager 1 flyby of Saturn's moon Titan the plasma wave instrument detected an intense band of low-frequency electric field noise [*Gurnett et al.*, 1981, 1982]. This noise occurred over the frequency range from about 10 Hz to 1 kHz and was most intense on the inbound pass shortly before closest approach. In this paper we investigate the origin of this noise and show that the noise is produced by a beam-plasma interaction between the corotating magnetosphere of Saturn and newly created ions from the atmosphere of Titan.

Titan is the only moon in the solar system known to have a substantial atmosphere. At the time of the Voyager 1 flyby, Titan was located within the outer magnetosphere of Saturn. The Voyager 1 measurements showed that Titan has no appreciable intrinsic magnetic field [*Ness et al.*, 1981]. Therefore its atmosphere interacts directly with the magnetosphere of Saturn. *Hartle et al.* [1982] described a model of this interaction, which is shown in Figure 1. The Voyager 1 trajectory, projected into the Saturnian equatorial plane, is indicated by the line labeled V1 trajectory near the bottom of the diagram. The intense low-frequency electric field noise occurs in the cross-hatched region from about 0532:30 to 0538:30 spacecraft event time (SCET). This noise was called sheath noise by Gurnett et al., because it is qualitatively similar to the electrostatic noise seen in the magnetosheath at earth and in the ionosheath at Venus [*Gurnett et al.*, 1982; *Rodriguez*, 1979; *Scarf et al.*, 1980]. A similar kind of noise was also observed near the upstream edge of the ionized gas clouds produced by the Active Magnetospheric Plasma Tracer Explorers (AMPTE) solar wind ion releases [*Gurnett et al.*, 1985, 1986]. In the AMPTE experiment the noise was explained by a beam-plasma interaction between the nearly stationary ions produced by the gas cloud and the rapidly flowing solar wind protons. The similarity of the Titan noise to the noise observed during the AMPTE ion releases leads us to suggest that the noise observed near Titan is generated by a similar type of interaction between the corotating plasma of Saturn's magnetosphere and the nearly stationary plasma created by ionization of Titan's atmosphere. In section 2 we summarize the observations related to the wave phenomena, and in section 3 we present a detailed analysis of the ion beam-plasma instability.

Paper number 6A8611.
0148-0227/87/006A-8611$05.00

2. SUMMARY OF OBSERVATIONS

The properties of the magnetospheric plasma just outside the wake region are fundamental to the understanding of the interaction of Saturn's magnetosphere with Titan's atmosphere. It has been known from the Voyager 1 experiments that there are at least two ion components, H^+ and N^+, in the magnetosphere near the orbit of Titan. In addition, N_2^+ and H_2CN^+ were also possibly present [*Hartle et al.*, 1982]. The basic properties of the magnetospheric plasma near the orbit of Titan are summarized by *Neubauer et al.* [1984]. The number density of protons, H^+, was about 0.1 cm^{-3}, and the number density of nitrogen ions, N^+, was about 0.2 cm^{-3}. The other possible components were minor and will be ignored in this analysis. The temperatures of the H^+ and N^+ ions were 210 eV and 2.9 keV, respectively. The electron number density and temperature were about 0.3 cm^{-3} and 200 eV. To a good approximation the plasma flow velocity was in the corotational direction (20° deflected toward Saturn), and the speed ranged from about 80 to 150 km/s, somewhat less than the corotational speed near Titan's orbit, which is 200 km/s.

Titan's exosphere has been studied in detail by *Hartle et al.* [1982]. The exosphere consists mainly of molecular nitrogen, N_2, and atomic hydrogen, H. The densities of N_2 and H were observed to be 10^8 cm^{-3} and 4×10^4 cm^{-3} at the exobase, which is 4000 km from the center of Titan (see Figure 1) [*Broadfoot et al.*, 1981]. Assuming a temperature of 160°K, *Hartle et al.* [1982] derived the radial density distributions shown in Figure 2. The density scale height of N_2 was about 150 km, and that of H was about 1500 km.

Upper hybrid resonance emissions observed in the vicinity of Titan provided a plasma density profile along the spacecraft trajectory. The top panel of Figure 3 shows the plasma density profile obtained from these emissions. This figure was reproduced from *Gurnett et al.* [1982]. The inbound sheath, the tail region, and the outbound sheath, if there is one, are indicated. The density level of the magnetospheric plasma, N^+ and H^+,

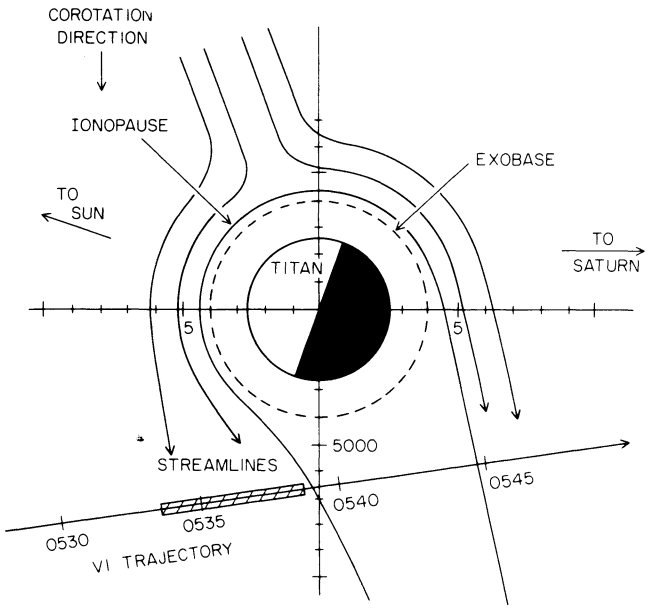

Fig. 1. The magnetospheric plasma flow around Titan and Voyager 1 trajectory, projected in the Saturnian equatorial plane. The electrostatic noise was observed in the crosshatched region. Since this noise occurs in a sheathlike region around Titan, it is called sheath noise.

which was about 0.3 cm^{-3}, is also indicated by the horizontal dashed line. As can be seen, the plasma density was strongly enhanced, up to about 40 cm^{-3}, in the vicinity of Titan. Since the plasma in the wake originated mostly from the photoionization of exospheric particles, the plasma density profile was basically governed by the exospheric density distribution. The scale height of the plasma density is about 500 km. The fractions of H^+ and N^+, or any other minor species, such as N_2^+ of H_2CN^+, are not known.

The low-frequency electric field intensities detected by the plasma wave spectrum analyzer are shown in the bottom panel of Figure 3. The sheath noise, which occurs from 0532:30 to 0538:30 SCET, is clearly distinguishable from the noise in the tail region, which occurs from 0539:30 to 0545:30 SCET. The sheath noise has a broad frequency range, from 10 to 1000 Hz. A representative spectrum of this noise is shown in Figure 4. The spectrum has a broad peak centered at a frequency of about 100–200 Hz. The broadband electric field strength is about 0.5 mV m^{-1}. As can be seen from Figure 3, the frequency of the sheath noise has a tendency to increase as the spacecraft approached Titan. During this time the plasma density increased monotonically along the trajectory. However, a clear cutoff is seen at about 0539:00 SCET, when the density is about 15–20 cm^{-3}. The intense noise was only observed on the inbound leg, which is on the dayside of Titan, and was essentially absent on the outbound leg, which is on the nightside.

3. Origin of the Sheath Noise

The plasma processes in Titan's wake are known to be complicated and involve ionization, mass loading, and ion acceleration. To try to understand the origin of the plasma wave noise, a simplified model will be used. This model is intended to represent the main features of the Titan-magnetospheric interaction in the region where the sheath noise occurred. Since the sheath noise was only detected during the time interval from 0532:30 to 0538:30 SCET, we

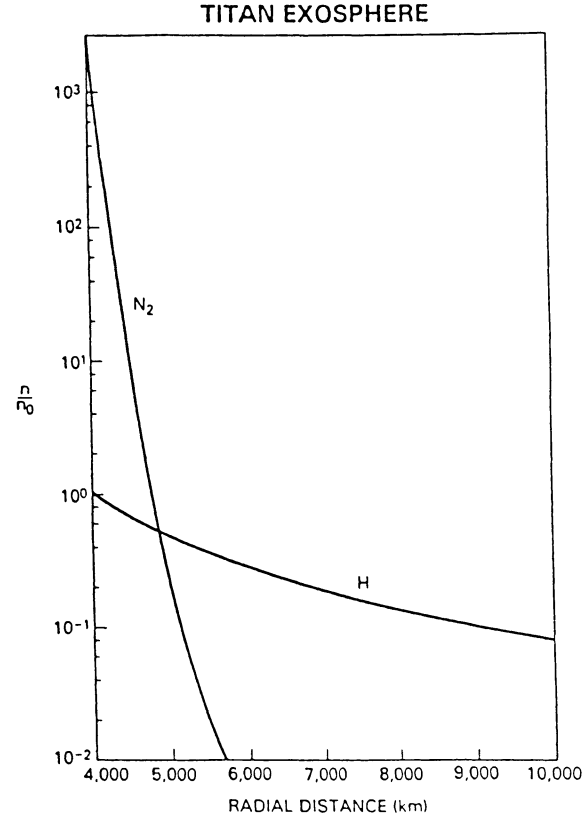

Fig. 2. The radial density distribution of Titan's exosphere, normalized by the density of H at the exobase, n_0 [*Hartle et al.*, 1982].

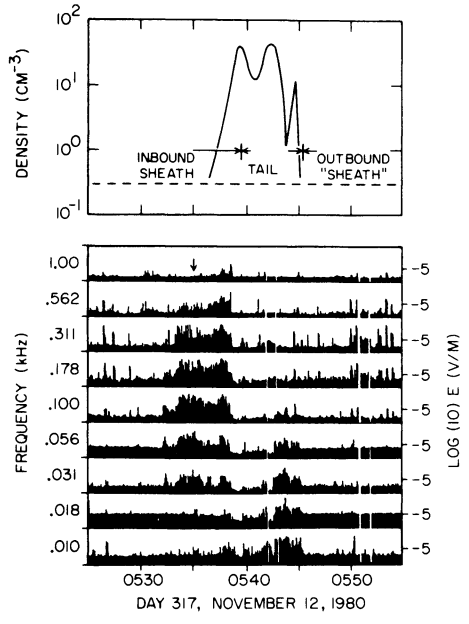

Fig. 3. The electron density profile along the Voyager 1 trajectory provided by upper hybrid resonance emissions (top panel) and the low-frequency electric field noise observed in the vicinity of Titan. The dashed line in the top panel indicates the total density of the magnetospheric plasma. The sheath noise appeared from 0532:30 to 0538:30 SCET, and tail noise appeared from 0539:30 to 0545:30 SCET.

will concentrate on the motions of particles in this region. There are basically three major groups of particles to be dealt with: (1) ions from the corotational magnetospheric plasma of Saturn, (2) ions from the exosphere of Titan, and (3) electrons. It is necessary to discuss the characteristics of each group, such as the composition, temperature, and velocity distribution.

First, it is known that the ions in the Saturnian magnetosphere are mostly H^+ and N^+. For the corotational magnetospheric plasma, Titan and its atmosphere act like an obstacle. However, this obstacle becomes ineffective at high altitudes, as the atmospheric density decreases. In the region where the sheath noise occurs, the ions from the corotational plasma stream through the atmosphere with only a slight interaction. This can be checked by noting that no shock existed in front of Titan and that the magnetic field differs only slightly from the field far away from Titan [see *Kivelson and Russell*, 1983; *Ness et al.*, 1982]. Therefore in our wave analysis we will treat the H^+ and N^+ ions in the corotational plasma as beams with drifting Maxwellian distributions. The drift velocity is taken to be the magnetospheric flow velocity, V_m. The densities and temperatures are the corresponding values for the magnetospheric plasma.

Second, we need to develop a model for the motion of the newly born ions from Titan's exosphere. Because of the weak gravitational acceleration in the upper atmosphere of Titan, neutral particles such as H, N, H_2, and N_2 escape by thermal and/or nonthermal processes [*Hunten et al.*, 1984]. These neutral particles are ionized by solar ultraviolet radiation, electron impact, and other mechanisms. The newly born ions have initial velocities that are approximately the same as the original velocities of the neutrals, basically the thermal velocities. Once ionized, they are accelerated by the corotational electric field **E** in the magnetospheric plasma. If the **B** field is in the minus z direction and the flow velocity is in the y direction, then the newly born ions move in cycloidal trajectories in the x-y plane more or less as shown in Figure 5 [*Hartle et al.*, 1982]. In the **B** field direction the ions move at the initial velocities. For such ions the velocity distributions are dependent on their cyclotron radii in comparison to the scale length

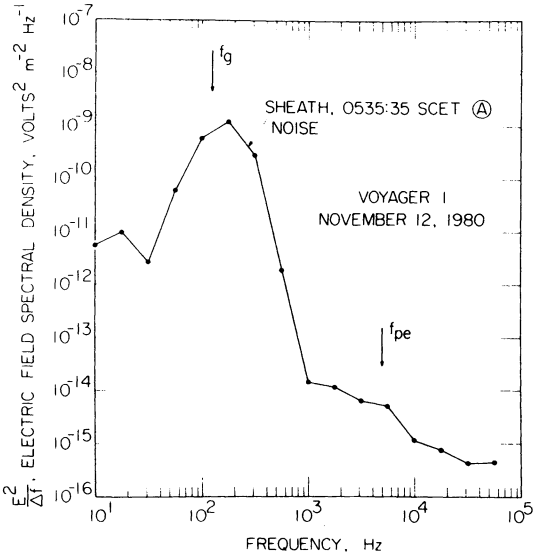

Fig. 4. The electric field spectral density of the sheath noise at the time marked by the arrow in Figure 3.

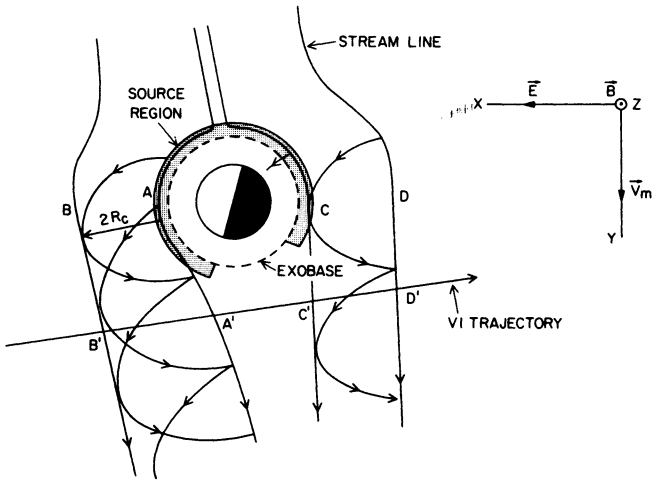

Fig. 5. Illustration of fields and particle motions. Right panel: if **B** is in $-z$ direction and the corotational velocity is in y direction, then the **E** field is in the x direction. Left panel: the main source region is shown by the darkened area, newly born ions have cycloidal trajectories, A-A′ and C-C′ are the streamlines near the main source region, and B-B′ and D-D′ are twice the N^+ gyroradius away.

of the plasma source. If the cyclotron radii of the ions are much smaller than the scale length and the thermal velocities are much less than the **E** × **B** drift velocity, then a ring-type distribution will be formed [see *Wu and Davidson*, 1972]. However, if the cyclotron radii of the ions are larger than the scale length of the plasma source, a ring-type distribution cannot be formed because the source is inhomogeneous. Since N^+ is believed to be one of the major components of the newly created ions, we can take it as an example to study the ion distributions in the x-y plane. The scale length (height) of N_2, which is the source of N^+, is about 150 km. This scale length is much smaller than the cyclotron radius of N^+, which is about 3470 km. As shown in Figure 5, the source region can be considered to be a thin layer near the top of the atmosphere. Two source regions exist, corresponding to streamlines that pass around the daysides and the nightsides of Titan. Ions originating from these two source regions behave quite differently. Ions produced on the dayside streamline, A-A′ in Figure 5, are accelerated away from Titan by the corotational electric field, **E**, producing cycloidal trajectories bounded by streamline A-A′ and B-B′, which is located 2 R_c outward from the source surface where R_c is the cyclotron radius of N^+ ions. This region of accelerated N^+ ions, between streamlines A-A′ and B-B′, is in good agreement with the region where the sheath noise is observed (compare with Figure 1). Ions produced on the nightside streamline, C-C′ in Figure 5, are accelerated toward Titan by the corotational electric field, where they are absorbed due to collisions with the atmosphere. Atmospheric collisions are effective for removing newly born ions out to streamline D-D′, which is located 2 R_c outward from the source surface. Although ions produced beyond D-D′ could escape, at these large distances from Titan the neutral gas density is so low that the source strength is negligible. Thus although a source exists for streamlines on the nightside of Titan, this source is not effective for injecting ions downstream of Titan. This asymmetry between the dayside and nightside explains why the sheath noise only occurs on the inbound pass.

Next we consider the velocity distribution function of the

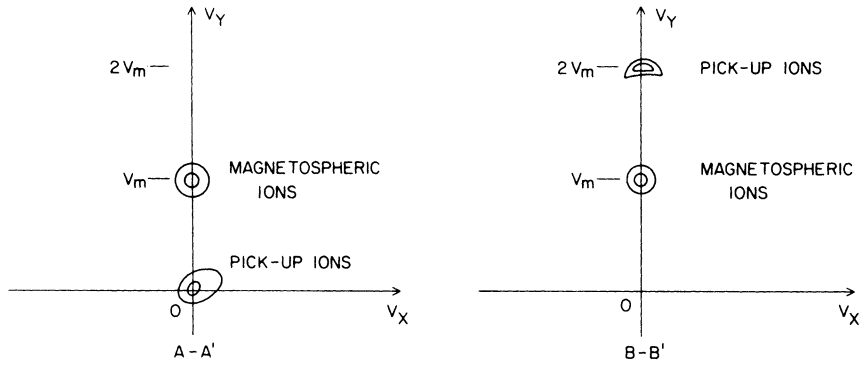

Fig. 6. Ion distribution along the A-A′ line and B-B′ line in Figure 5. The magnetospheric ions have drift velocity of $\mathbf{V}_m$. The pickup ions from Titan's exosphere have distributions peaked at the origin along A-A′ but peaked at $2V_m y$ along B-B′.

newly born ions. Ions created near streamline A-A′ have very small velocities. These ions are accelerated in the x direction due to the **E** field and gyrate about the z direction due to the **B** field. When they reach the B-B′ streamline, the x component of velocities goes to zero, and the y component becomes $2V_m$, which is twice the flow velocity of the corotational magnetospheric plasma. The x component of the velocity then reverses, and ions move back toward the A-A′ streamline. As they approach the A-A′ line, the ions become nearly stationary and then start another cycle. Along the A-A′ line the most newly created ions have small velocities, and their distribution is similar to the distribution of neutrals from which the ions were born. Such a distribution is qualitatively illustrated in the left panel of Figure 6. The newly created ions, also called pickup ions, are located at the origin. The magnetospheric ion distribution peaks at the velocity $V_m\hat{y}$. The right panel of Figure 6 shows ion distributions along the B-B′ line. Since the majority of the pickup ions have small x components of velocities and their y components are close to $2V_m$, their distribution function peaks at $2V_m\hat{y}$. The distribution of the magnetospheric ions is similar to that along the A-A′ line. Ions with different masses have different cyclotron radii. Therefore the B-B′ line defined above for N^+ ions is not suitable for H^+ and $N_2{}^+$. But the distributions for different species of newly born ions along the A-A′ line should be very similar. More complicated distributions with multiple peaks occur in the region between the A-A′ and B-B′ lines. Because of the complexity we will not consider these more complicated distributions in the present analysis. For simplicity we assume that the distribution function of the pickup ions is a Maxwellian. The temperature of the pickup ions should be close to the exospheric temperature, which is about 186°K.

Third, it is necessary to find a reasonable way to deal with the electrons. First of all, there are probably two groups of electrons, hot electrons associated with the magnetospheric plasma and cold electrons associated with the newly ionized exospheric plasma. The hot electron temperature, $T_e{}^h$, can be taken as 200 eV, which is the temperature of the magnetospheric plasma. The cold electrons are produced by photoionization of the exospheric gas. The cold electron temperature, $T_e{}^c$, has been determined to vary from 4.6 eV to 44 eV [*Eviatar et al.*, 1982]. However, we will take a wider range from 2 eV to 200 eV. The lower limit is the temperature that would result from photoionization by ultraviolet light, and the upper limit takes into account the possible heating of the photoelectrons up to the magnetospheric temperatures. The next issue is the bulk motion of the electrons. It is known that in addition to the gyrations around the magnetic field lines, the electrons move according to the **E** × **B** drift. In the region far from Titan the electrons and the ions drift together with the same velocity. However, in Titan's vicinity, where there are electrons associated with the newly born ions, the situation is different. Because of the quick response of the electrons to the convection electric field, electrons with different origins are not distinguishable. Therefore all electrons should drift together. Now the question is, do they drift with the same velocity as the corotational magnetospheric ions, or with the same velocity as the newly born exospheric ions, or at some intermediate velocity? Estimates of the current rule out the first two possibilities. Magnetic field measurements show that the change in **B** from 0532:30 to 0538:30 SCET is not more than 2 nT [*Ness et al.*, 1982; *Neubauer et al.*, 1984]. The spacecraft traveled about 6000 km during this time interval. The current density in the sheath region can be estimated using $J \simeq (1/\mu_0)(\Delta B/\Delta l)$, where ΔB is the **B** field change, Δl is the distance, and $\mu_0 = 4\pi \times 10^{-7}$ henry/m is the permeability of free space. The current density estimated from this procedure is about 2.7×10^{-10} A/m^2. If we take the measured ion densities and let the electrons drift with either group of ions, the current density would be at least 1 order of magnitude higher and would produce a magnetic field change at least 1 order of magnitude higher than is observed. Therefore the only possible case is that the electrons drift with an intermediate velocity. We will assume that this intermediate drift velocity is such that the total current is zero. Although this assumption may not be precisely correct, it is a reasonable first-order approximation. From the zero current condition it is relatively easy to show that the electron drift velocity is given by

$$V_d = \frac{N_b V_m}{N_b + N_s} \tag{1}$$

where V_m is the magnetospheric flow velocity and N_b and N_s are the densities of the magnetospheric and exospheric ions, respectively.

In summary, the model for the wave analysis is illustrated in Figure 7. This model is appropriate for the region near the A-A′ line in Figure 5. A close relation can be found to the region near the B-B′ line and will be discussed later. The curves are not drawn to scale for purpose of clarity. Six species of ions are considered. Each species is assumed to have a drifting Maxwellian distribution. A summary of all parameters and their assumed values is given in Table 1.

It is obvious from Figure 7 that the ion velocity distribution function has two peaks. Double-humped velocity distributions of this type are known to be unstable and rapidly lead to the generation of intense electrostatic waves [*Penrose*, 1960]. Ion beam instabilities of the type illustrated in Figure 7 were first analyzed in detail by *Fried and Wong* [1966] and were analyzed in further detail by *Gurnett et al.* [1985] to interpret the low-frequency electrostatic noise observed in the AMPTE solar wind lithium releases. For a multispecies unmagnetized plasma and electrostatic instability is determined by the reduced distribution function,

$$F(v) = \sum_s \frac{m_e}{m_s} F_s(v) \tag{2}$$

where m_s and $F_s(v)$ are the mass and distribution function of sth species and m_e is the electron mass. The summation is over all species. The plasma is unstable when $F(v)$ is sufficiently double-humped to satisfy the Penrose criterion [*Krall and Trivelpiece*, 1973]. As can be seen from Figure 7, instabilities are in principle possible for phase velocities between 0 and V_d and between V_d and V_m. However, the thermal velocity of the magnetospheric ions is about equal to V_m, which is larger than $V_m - V_d$. Therefore the instability between V_d and V_m cannot occur because the magnetospheric ion distribution is too broad to produce a double hump. Instability can only occur in association with the relatively cold exospheric ions at phase velocities between 0 and V_d.

Before proceeding with the analysis we will consider the effect of the magnetic field. In the present problem the magnetic field is essentially perpendicular to the plane of Titan's orbit and therefore to the plasma flow direction. Its magnitude is about 5 nT. The electron cyclotron frequency is about 140 Hz. The cyclotron frequency of a proton is less than 0.1 Hz, and that of an N^+ ion is even less. The wave frequency we consider here is much larger than the ion cyclotron frequency. Therefore the effect of the magnetic field on the ion motions is negligible. The electron cyclotron frequency is almost in the middle of the wave frequency range. In general, electrons should be treated as magnetized. However, the cyclotron radius of the thermal electrons is 9.5 km [*Neubauer et al.*, 1984]. Even for photoelectrons the cyclotron radius is of the order of 1 km. It is anticipated that the wavelength of the electrostatic noise will be short, probably only several tens of meters. For such short wavelengths, much less than the cyclotron radius, the wave motion is basically not affected by the magnetic field. The theoretical proof of this result was given by *Stepanov* [1959]. Therefore we will neglect the magnetic field in the calculation and verify the consistency afterward.

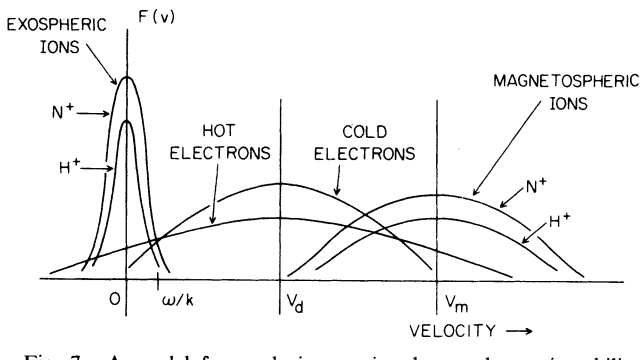

Fig. 7. A model for analyzing an ion beam–plasma instability. The magnetospheric H^+ and N^+ ions flow with speed V_m, and electrons (hot and cold) drift with speed V_d; the newly created ions are nearly stationary. The curves are not drawn to scale.

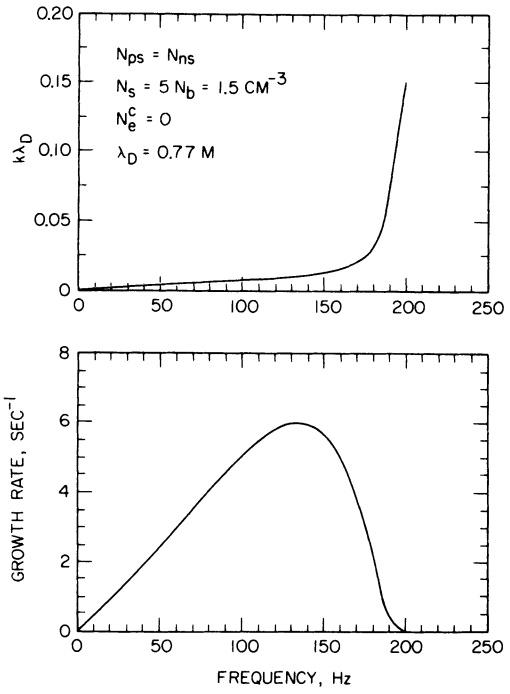

Fig. 8. Plots of the growth rate, γ, and normalized wave number, k, as a function of frequency under the conditions $N_s = 5N_b = 1.5$ cm^{-3}, $N_{ns} = N_{ps}$, and $N_e{}^c = 0$.

The linearized electrostatic wave dispersion relation for a multispecies plasma with no magnetic field is given by

$$D(k, \omega) = 1 - \sum_s \frac{\omega_s{}^2}{k^2} \int \frac{\partial F_s/\partial v}{v - \omega/k}\, dv = 0 \tag{3}$$

where k is the projection of wave number in the beam direction, ω is the complex frequency whose real part gives the frequency and imaginary part gives the growth rate for the instability, and ω_s is the plasma frequency for sth species. If $F_s(v)$ is a Maxwellian distribution, the dispersion equation (3) can be written

$$D(k, \omega) = 1 - \frac{1}{2} \sum_s \frac{1}{(k\lambda_{Ds})^2} Z'(z_s) = 0 \tag{4}$$

where λ_{Ds} is the Debye length for sth species, Z' denotes the derivative of the plasma dispersion function [see *Fried and Conte*, 1961], and z_s is

$$z_s = \left(\frac{\omega}{k} - V_s\right) \Big/ a_s \tag{5}$$

where a_s and V_s are the thermal and drift velocities of sth species, respectively. The dispersion equation is solved numerically by using Salzer's method to evaluate the plasma dispersion function and Muller's method for root-finding [*Fried and Conte*, 1961; *Salzer*, 1951; *Muller*, 1956].

Figure 8 shows a representative growth rate for the ion-beam plasma instability. The top panel shows the wave number, k, normalized by the Debye length, λ_D, as a function of frequency. The bottom panel shows the growth rate, γ, versus frequency. The parameters used here are as follows:

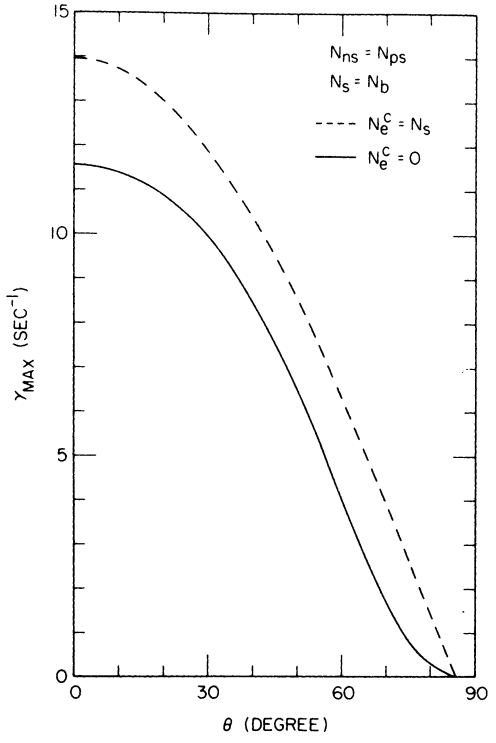

Fig. 9. The maximum growth rates as a function of θ and the angle between $\mathbf{k}$ and $\mathbf{V}_m$ under the conditions $N_{ns} = N_{ps}$ and $N_s = N_b$. The solid curve is for the case $N_e^c = 0$, and the dashed curve is for $N_e^c = N_s$.

$N_{ps} = N_{ns}$, $N_s = 5 \times N_b = 1.5$ cm^{-3}, $T_e^c = 200$ eV, $N_e^c = 0$, and $N_e^h = N_s + N_b$. The remaining parameters are given in Table 1. With the above parameters the Debye length is computed to be about 0.77 m. Taking $k\lambda_D$ to be 0.05 or higher, the wavelength is estimated to be about 20 m or less. This wavelength is consistent with the assumption that the magnetic field can be neglected. As seen in Figure 8, the growth rate is very high, up to 6 s^{-1}, which means that a wave disturbance can grow 1000 times in 1 s. At Voyager 1's closest approach the radial distance to the center of Titan was about 6500 km. As is shown in Figure 1, the unstable region on the upstream side of the spacecraft path has the scale size of at least 6500 km. The wave encountered by the spacecraft must start growing in this region and is then carried downstream along with the plasma flow. If a wave starts 1000 km upstream of the spacecraft path, for example, it takes 5 s (at a speed of 200 km/s, including the wave propagation) to reach the spacecraft. During this time the wave grows by a factor of 10^{15}, which is more than enough to grow from a thermal level to very high amplitudes. The frequency range, up to 200 Hz, agrees very well with the spectrum in Figure 4.

TABLE 1. Summary of Parameters

Quantities	Notations	Values
H^+ density in beam	N_{pb}	0.1 cm^{-3}
N^+ density in beam	N_{nb}	0.2 cm^{-3}
Total density in beam	N_b $(= N_{pb} + N_{nb})$	0.3 cm^{-3}
Newly created H^+ density	N_{ps}	Variable
Newly created N^+ density	N_{ns}	Variable
Total newly created density	N_s $(= N_{ps} + N_{ns})$	Variable
H^+ temperature in beam	T_{pb}	210 eV
N^+ temperature in beam	T_{nb}	2.9 eV
Exospheric H^+ temperature	T_{ps}	186°K
Exospheric N^+ temperature	T_{ns}	186°K
Hot electron temperature	T_e^h	200 eV
Cold electron temperature	T_e^c	2 eV ~ 200 eV
Beam velocity	V_m	150 km/s
Electron drift velocity	V_d	Variable
Cold electron density	N_e^c	Variable
Hot electron density	N_e^h	Variable

For the calculations in Figure 8 the wave vector, $\mathbf{k}$, is assumed to be parallel to the beam velocity. It can be shown that for the assumed parameters a wave propagating parallel to the beam velocity has the highest growth rate. Figure 9 gives the maximum growth rate, γ_{max} (maximized over $|\mathbf{k}|$), as a function of θ, the angle between $\mathbf{k}$ and $\mathbf{V}_m$ under the condition $N_{ps} = N_{ns}$ and $N_s = N_b$. The solid curve is for the case of no cold electrons, and the dashed curve is for the case $N_e^c = N_s$. As can be seen in the figure, the growth rates for both cases decrease monotonically as θ increases, and the instability ceases at about 85°. Similar results are obtained for all the conditions listed in Table 1. Therefore in the rest of the study we will consider the most unstable case, that is, $\theta = 0$.

In order to study the effect of the plasma density on the instability the marginal instability condition ($\gamma = 0$) has been investigated as a function of the plasma-beam density ratio, N_s/N_b. Figures 10 and 11 show the frequency of marginal instability as a function of density ratio, N_s/N_b. The dashed curves in these plots show the frequencies corresponding to the maximum growth rates. Figures 12 and 13 show the maximum growth rate versus N_s/N_b. The conditions for Figures 10 and 12 are $N_{ns} = N_{ps}$, $T_e^c = T_e^h = 200$ eV, $N_e^c = 0$, and $N_e^h = N_s + N_b$. The conditions for Figures 11 and 13 are $N_{ns} = N_{ps}$, $T_e^h = 200$ eV, $T_e^c = 2$ eV, $N_e^c = N_s$, and $N_e^h = N_b$. The parameters not mentioned take the values given in Table 1. These two groups of figures cover the two extreme limits for the electron temperatures. The two extremes give very similar results. As can be seen in Figures 12 and 13, the maximum growth rates reach about 10 s^{-1}, which is quite high. The frequency range extends up to several hundred hertz which is in good agreement with the observed frequency range. One important feature shown in Figures 10 and 11 is that the instability only occurs for a limited range of density ratio, N_s/N_b, between about 0.001 and 50 for $N_e^c = 0$ and between about 0.001 and 25 for $N_e^c = N_s$. This condition shows that the instability cannot occur far from Titan, where

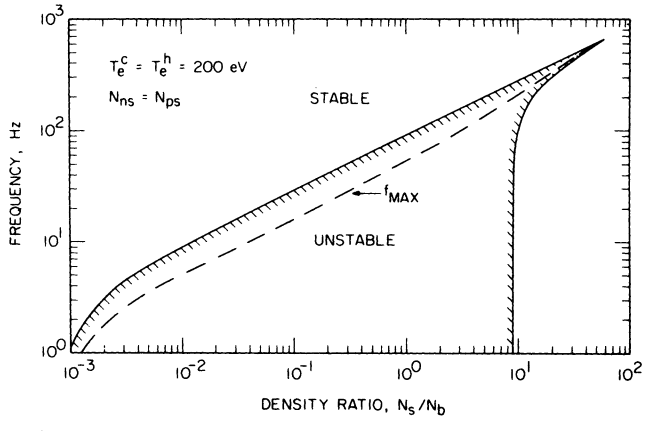

Fig. 10. The frequency of marginal stability, $r = 0$, as a function of the density ratio, N_s/N_b, assuming $N_{ns} = N_{ps}$ and $N_e^c = 0$. The dashed curve indicates the frequency associated with the maximum growth rate.

the newly created plasma density is too high. The effect of the different fractions of N^+ and H^+ on the instability has been studied. The results are similar to Figures 10–13 except that more protons give a slightly larger frequency range.

Since the Voyager 1 trajectory is almost perpendicular to the streamlines, which are in the **k** direction, the Doppler shift due to the motion of the spacecraft is negligible. In other words, the frequency from the above analysis should be directly compared with the frequency detected by the spacecraft.

The model illustrated in Figure 5 and the wave analysis based on it apply to the region near streamline A-A′, which is a representative streamline passing through the source region. The electrostatic waves occurring in this region are generated by the interaction of the magnetospheric ions streaming through the newly created plasma. The free energy is provided by the relative motion between the magnetospheric ions and the newly born exospheric ions. The sharp cutoff at about 0538:30 in Figure 3 indicates that the instability ceases at this point. This cutoff probably occurs because the exospheric plasma density exceeds the density limit for the instability, $N_s/N_b \gtrsim 50$. In addition, the plasma flow velocity in the region between the streamlines A-A′ and C-C′ is significantly reduced [see *Neubauer*, 1984]. This causes the magnetospheric ions, as a beam, to be insufficient to drive an instability. This could be another reason for the cutoff.

As seen in Figure 6, the ion distribution along the B-B′ line is just the reflection of the distributions along the A-A′ line about $Vy = V_m$. Therefore if we choose a frame of reference which moves with velocity of $2V_m\hat{y}$ relative to the frame in Figure 6 and let **k** be opposite to the streamline direction, we obtain a model that is the same as that in Figure 7. Similar kinds of instability analyses can be performed. In fact, a corresponding relation between the same modes in the A-A′ case and the B-B′ case can be found. For example, if an unstable mode with frequency ω' and phase velocity V_p' is detected by the spacecraft along streamline A-A′, the corresponding mode detected by the spacecraft along streamline B-B′ will have a frequency

$$\omega = \omega'\left|1 - \frac{2V_m}{V_p'}\right| \tag{6}$$

This wave propagates with **k** in the streamline direction. Because of the existence of such a corresponding relation the conditions for the instability in the B-B′ case are the same as

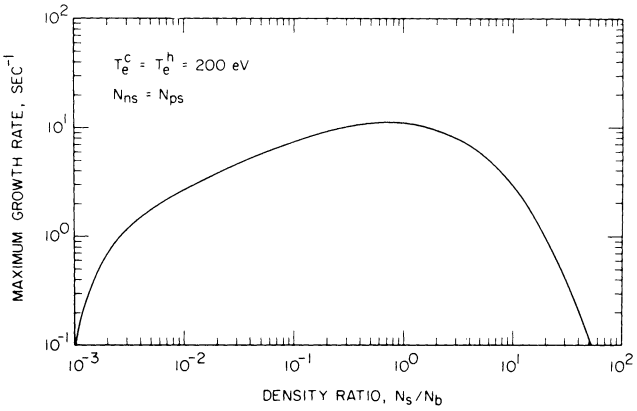

Fig. 12. The maximum growth rate as a function of the density ratio, N_s/N_b, for the case in Figure 10.

those in the A-A′ case. However, the frequency range is different. Depending on the density ratio, N_s/N_b, ω could be very close to ω' or an order of magnitude higher than ω'. The reason is that V_p' can be very close to V_m in some cases, or just a few kilometers per second, which is an order of magnitude smaller than V_m. In either case the frequency range is still in good agreement with the observations. In fact, the pickup ion density, N_s, in the B-B′ case is much less than that in the A-A′ case. The consequence, as can be seen from Figures 10 and 11, is that the frequency range for ω' in the B-B′ case is much less than that in the A-A′ case. This effect cancels the increase of the actual frequency ω by the Doppler shift so the ω in the B-B′ case is still lower. Similar to the situation along A-A′ the free energy along B-B′ is also provided by the relative motion between the magnetospheric ions and the pickup ions, although in this case the pickup ions have been accelerated to a velocity of $2V_m$.

Although the intermediate region between A-A′ and B-B′ has not been analyzed, the same basic type of instability should also exist in this region. The **k** vector directions for maximum growth in this intermediate region are in general not aligned with the plasma flow, so the Doppler shift is intermediate between the A-A′ and B-B′ cases. Also, because the cycloidal trajectories cross and different ion species are accelerated to different velocities, multiple ion beams will be present which will excite a more complex wave vector and frequency distribution.

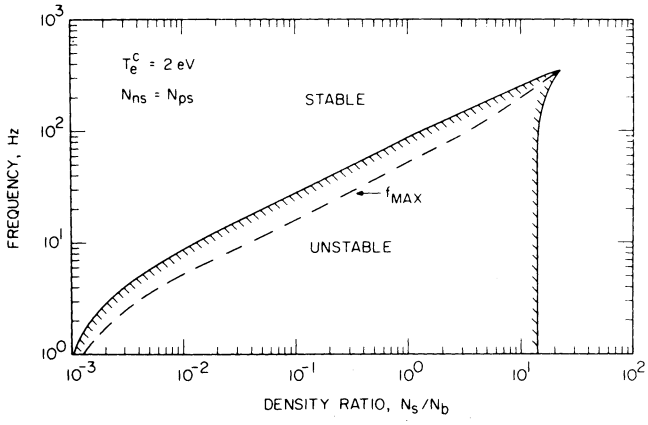

Fig. 11. The same plot as in Figure 10 with $N_e^c = N_s$ and $T_e^c = 2$ eV.

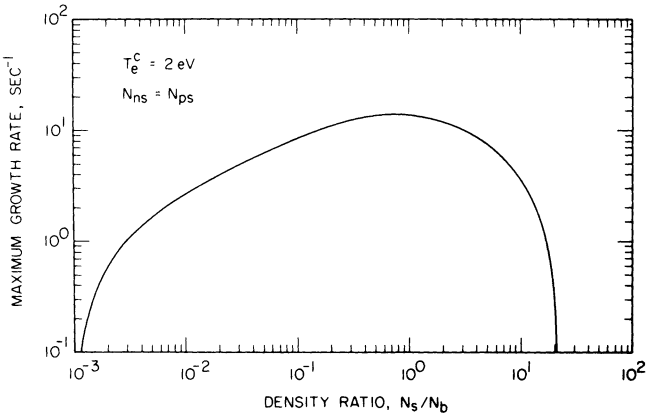

Fig. 13. The maximum growth rate as a function of the density ratio, N_s/N_b, for the case in Figure 11.

4. CONCLUSION

The low-frequency electric field noise observed by Voyager 1 during the inbound crossing of Titan's wake has been analyzed in detail. The analysis shows that the noise is generated by an ion beam-plasma instability caused by the corotational magnetospheric ions, mostly H^+ and N^+, streaming through plasma produced by photoionization of Titan's exosphere. This mechanism explains the basic features of the noise. By using known (measured) and reasonably assumed parameters, one gets high growth rates and good agreement with the observed frequency range. The instability has a limited range for the beam to plasma density ratio, N_s/N_b, from about 0.001 to 50. A simple model for the cycloidal exospheric ion trajectory explains why the noise only occurs in a limited area along the V1 trajectory and why the noise only occurs on the inbound pass.

However, some detailed aspects of the noise cannot be explained because of the lack of some information and the complexity of the Titan-magnetospheric interaction. For instance, the calculated frequency for the maximum growth rate does not match the observations in detail, and also the calculated frequency range for the particular density ratio does not follow the observed density exactly. In some cases the processes in the interaction region are not well known. In particular, the particle distributions in the inbound wake are probably more complicated than has been assumed, and further studies are required. Also, for the very high growth rates found, nonlinear effects will always be present. Nonlinear effects stabilize the system, saturate the wave growth, and broaden the frequency spectrum. Therefore a simple linear theory is not expected to explain the sheath noise completely. Plasma simulations will eventually be required to fully investigate the nonlinear effects, including the role of these waves in heating the plasma.

A similar kind of noise was also observed in the vicinity of the space shuttle [*Shawhan et al.*, 1984], apparently caused by an interaction of gases from the shuttle with the surrounding ionosphere. This type of noise seems to be a common phenomena when a neutral gas interacts with a rapidly moving plasma.

Acknowledgments. This research was supported by NASA through grant NGL 16-001-043 with NASA Headquarters and contract 954013 with the Jet Propulsion Laboratory and by the Office of Naval Research through contract N00014-85-K-0404.

The Editor thanks P. Rodriguez and two other referees for their assistance in evaluating this paper.

REFERENCES

Bridge, H. S., J. W. Belcher, A. J. Lazarus, S. Olbert, J. D. Sullivan, F. Bagenal, P. R. Gazis, R. E. Hartle, K. W. Ogilvie, J. D. Scudder, E. C. Sittler, A. Eviatar, G. L. Siscoe, C. K. Goertz, and V. M. Vasyliunas, Plasma observations near Saturn: Initial results from Voyager 1, *Science*, *212*, 217, 1981.

Broadfoot, A. L., B. R. Sandel, D. E. Shemansky, J. D. Holberg, G. R. Smith, D. F. Strobel, J. C. McConnell, S. Kumar, D. M. Hunten, S. K. Atreka, T. M. Donahue, H. W. Moos, J. L. Bertaux, J. E. Blamont, R. B. Pomphrey, and S. Linick, Extreme ultraviolet observations from Voyager 1 encounter with Saturn, *Science*, *212*, 206, 1981.

Eviatar, A., G. L. Siscoe, J. D. Scudder, E. C. Sittler, Jr., and J. D. Sullivan, The plumes of Titan, *J. Geophys. Res.*, *87*, 8091, 1982.

Fried, B. D., and S. D. Conte, *The Plasma Dispersion Function*, Academic, Orlando, Fla., 1961.

Fried, B. D., and A. Y. Wong, Stability limits for long longitudinal waves in ion beam–plasma interactions, *Phys. Fluids*, *9*, 1084, 1966.

Gurnett, D. A., W. S. Kurth, and F. L. Scarf, Plasma waves near Saturn: Initial results from Voyager 1, *Science*, *212*, 239, 1981.

Gurnett, D. A., F. L. Scarf, and W. S. Kurth, The structure of Titan's wake from plasma wave observations, *J. Geophys. Res.*, *87*, 1395, 1982.

Gurnett, D. A., R. R. Anderson, B. Häusler, G. Haerendel, O. H. Bauer, R. A. Treumann, H. C. Koons, R. H. Holzworth, and H. Lühr, Plasma waves associated with the AMPTE artificial comet, *Geophys. Res. Lett.*, *12*, 851, 1985.

Gurnett, D. A., T. Z. Ma, R. R. Anderson, O. H. Bauer, G. Haerendel, B. Häusler, G. Paschmann, R. A. Treumann, H. C. Koons, R. Holzworth, and H. Lühr, Analysis and interpretation of the shocklike electrostatic noise observed during the AMPTE solar wind lithium releases, *J. Geophys. Res.*, *91*, 1301, 1986.

Hartle, R. E., E. C. Sittler, Jr., K. W. Ogilvie, J. D. Scudder, A. J. Lazarus, and S. K. Atreya, Titan's ion exosphere observed from Voyager 1, *J. Geophys. Res.*, *87*, 1383, 1982.

Hunten, D. M., M. G. Tomasko, F. M. Flasar, R. E. Samuelson, D. F. Strobel, and D. J. Stevenson, Titan, in *Saturn*, edited by T. Gehrels and M. S. Matthews, pp. 671–759, The University of Arizona Press, Tucson, 1984.

Kivelson, M. G., and C. T. Russell, The interaction of flowing plasma with planetary ionospheres: A Titan-Venus comparison, *J. Geophys. Res.*, *88*, 49, 1983.

Krall, N. A., and A. W. Trivelpiece, *Principles of Plasma Physics*, p. 473, McGraw-Hill, New York, 1973.

Muller, D. E., A method for solving algebraic equations using an automatic computer, *Math. Comput.*, *10*, 208, 1956.

Ness, N. F., M. H. Acuña, R. P. Lepping, J. E. P. Connerney, K. W. Behannon, L. F. Burlaga, and F. M. Neubauer, Magnetic field studies by Voyager 1; Preliminary results at Saturn, *Science*, *212*, 211, 1981.

Ness, N. F., M. H. Acuna, K. W. Behannon, and F. M. Neubauer, The induced magnetosphere of Titan, *J. Geophys. Res.*, *87*, 1369, 1982.

Neubauer, F. M., D. A. Gurnett, J. D. Scudder, and R. E. Hartle, Titan's magnetospheric interaction, in *Saturn*, edited by T. Gehrels and M. S. Matthews, pp. 760–781, The University of Arizona Press, Tucson, 1984.

Penrose, O., Electrostatic instability of a uniform non-Maxwellian plasma, *Phys. Fluids*, *3*, 258, 1960.

Rodriguez, P., Magnetosheath electrostatic turbulence, *J. Geophys. Res.*, *84*, 917, 1979.

Salzer, H. E., Formulas for calculating the error function of a complex variable, *Math. Tables*, 67, 1951.

Scarf, F. L., W. W. L. Taylor, C. T. Russell, and R. C. Elphic, Pioneer Venus plasma wave observations: The solar wind–Venus interaction, *J. Geophys. Res.*, *85*, 7599, 1980.

Shawhan, S. D., G. B. Murphy, and J. S. Pickett, Plasma diagnostics package initial assessment of the shuttle orbiter environment, *J. Spacecr. Rockets*, *21*, 387, 1984.

Stepanov, K. N., Low-frequency oscillations of a plasma in a magnetic field, *Sov. Phys. JETP, Engl. Transl.*, *35(8)*, 808, 1959.

Wu, C. S., and R. C. Davidson, Electromagnetic instabilities produced by neutral-particle ionization in interplanetary space, *J. Geophys. Res.*, *77*, 5399, 1972.

C. K. Goertz, D. A. Gurnett, and T. Z. Ma, Department of Physics and Astronomy, The University of Iowa, Iowa City, IA 52242.

(Received June 20, 1986;
revised April 29, 1987;
accepted May 1, 1987.)